Calculating anisotropic physical properties from texture data using the MTEX open-source package

DAVID MAINPRICE[1]*, RALF HIELSCHER[2] & HELMUT SCHAEBEN[3]

[1]*Geosciences Montpellier UMR CNRS 5243, Université Montpellier 2, 34095 Montpellier Cedex 05, France*

[2]*Fakultät für Mathematik, Technische Universität Chemnitz, 09126 Chemnitz, Germany*

[3]*Mathematische Geologie und Geoinformatik, Institut für Geophysik und Geoinformatik, Technische Universität Freiberg, 09596 Freiberg, Germany*

Corresponding author (e-mail: David.Mainprice@gm.univ-montp2.fr)

Abstract: This paper presents the background for the calculation of physical properties of an aggregate from constituent crystal properties and the texture of the aggregate in a coherent manner. Emphasis is placed on the important tensor properties of 2nd and 4th rank with applications in rock deformation, structural geology, geodynamics and geophysics. We cover texture information that comes from pole figure diffraction and single orientation measurements (electron backscattered diffraction or EBSD, electron channelling pattern, Laue pattern, optical microscope universal-stage). In particular, we provide explicit formulae for the calculation of the averaged tensor from individual orientations or from an orientation distribution function (ODF). For the latter we consider numerical integration and an approach based on the expansion into spherical harmonics. This paper also serves as a reference paper for the mathematical tensor capabilities of the texture analysis software MTEX, which is a comprehensive, freely available MatLab toolbox that covers a wide range of problems in quantitative texture analysis, for example, ODF modelling, pole figure to ODF inversion, EBSD data analysis and grain detection. MTEX offers a programming interface which allows the processing of involved research problems as well as highly customizable visualization capabilities; MTEX is therefore ideal for presentations, publications and teaching demonstrations.

The estimation of physical properties of crystalline aggregates from the properties of the component crystals has been subject of extensive literature since the classical work of Voigt (1928) and Reuss (1929). Such an approach is only feasible if the bulk properties of the crystals dominate the physical property of the aggregate and the effects of grain-boundary interfaces can be ignored. For example, the methods discussed here cannot be applied to the electrical properties of water-saturated rock, where the role of interfacial conduction is likely to be important. Many properties of interest to earth and materials scientists can be evaluated from the knowledge of the single-crystal tensors and the orientation distribution function (ODF) of crystals in an aggregate, for example, thermal diffusivity, thermal expansion, diamagnetism and elastic wave velocities.

The majority of rock-forming minerals have strongly anisotropic physical properties and many rocks also have strong crystal preferred orientations (CPOs, or textures as they are called in materials science; these terms are used interchangeably in this paper as no possible confusion can result in present context) that can be described concisely in a quantitative manner by the *orientation distribution function* ODF. The combination of strong CPOs and anisotropic single-crystal properties results in a three-dimensional variation in rock properties. Petrophysical measurements are usually made under hydrostatic pressure and often at high temperatures to simulate conditions in the Earth, where presumably the micro-cracks present at ambient conditions are closed. The necessity to work at high pressure and temperature conditions limits the number of orientations that can be measured. Typically, three orthogonal directions are measured parallel to structural features, such as the lineation and foliation normal defined by grain shape. The evaluation of physical properties from CPO allows the determination of properties over the complete orientation sphere of the specimen reference frame.

This paper is designed as a reference paper for earth and material scientists who want to use the texture analysis software MTEX to compute

physical tensor properties of aggregates from constituent crystal properties and the texture of the aggregate. MTEX is a comprehensive, freely available MatLab toolbox that covers a wide range of problems in quantitative texture analysis, for example: ODF modelling, pole figure to ODF inversion, electron backscatter diffraction (EBSD) data analysis and grain detection. The MTEX toolbox can be downloaded from http://mtex.googlecode. com. Unlike many other texture analysis software, it offers a programming interface which allows for the efficient processing of complex research problems in the form of scripts (M-files). The MatLab environment provides a wide variety of high-quality graphics file formats to aid publication and display of the results. In addition the MTEX toolbox will work identically on Microsoft Windows, Apple Mac OSX and Linux platforms in 32 and 64 bit modes with a simple installation procedure.

In MTEX texture analysis information such as ODFs, EBSD data and pole figures are represented by variables of different types. For example, in order to define a unimodal ODF with half-width $10°$, preferred orientation $10°$, $20°$, $30°$ Euler angles and cubic crystal symmetry, the command

```
myODF = unimodalODF(orientation('Euler',
   10*degree, 20*degree,30*degree),
   ... symmetry ('cubic'), 'halfwidth',
   10*degree)
```

is issued which generates a variable myODF of type ODF, displayed as

```
myODF = ODF
   specimen symmetry: triclinic
   crystal symmetry : cubic

   Radially symmetric portion:
     kernel: de la Vallee Poussin, hw = 10
     center: (10, 20, 30)
     weight: 1
```

We will use this style of displaying input and output to make the syntax of MTEX as clear as possible. Note that there is also an exhaustive interactive documentation included in MTEX, which explains the syntax of each command in detail.

The outline of the paper is as follows. In the first section the basics of tensors mathematics and crystal geometry are briefly described and presented in terms of MTEX commands. In the second section these basics are discussed for some classical second-order tensors and the elasticity tensors. In particular, we give a comprehensive overview about elastic properties that can be computed directly from the elastic stiffness tensor. All calculations are accompanied by the corresponding MTEX commands. In the third section we are concerned with the calculation of average matter tensors from their single-crystal counterparts and

the texture of the aggregate. Here we consider textures given by individual orientation measurements, which lead to the well-known Voigt, Reuss and Hill averages, as well as textures given by ODFs, which lead to formulae involving integrals over the orientation space. We can compute these integrals in several ways: either we use known quadrature rule, or we compute the expansion of the rotated tensor into generalized spherical harmonics and apply Parseval's theorem. Explicit formulae for the expansion of a tensor into generalized spherical harmonics and a proof that the order of the tensor defines the maximum order of this expansion is included in the Appendix.

Tensor mathematics and crystal geometry

In what follows we give the necessary background to undertake physical property calculation for single crystals, without the full mathematical developments that can be found elsewhere (e.g. Nye 1985). We will restrict ourselves to linear physical properties, which are properties that can be described by a linear relationship between cause and effect such as stress and strain for linear elasticity.

Tensors

Mathematically, a tensor T of rank r is a r-linear mapping which can be represented by an r-dimensional matrix $T_{i_1,i_2,...,i_r}$. A rank zero tensor is simply a scalar value, a rank-one tensor T_i is a vector and a rank-two tensor T_{ij} has the form of a matrix. Linearity means that the tensor applied to r vectors $x^1, \ldots, x^r \in \mathbb{R}^3$, defines a mapping

$$(x^1, \ldots, x^r) \longrightarrow \sum_{i_1=1}^{3} \sum_{i_2=1}^{3} \cdots \sum_{i_r=1}^{3} T_{i_1,...,i_r} x^1_{i_1} \cdots x^r_{i_r}$$

which is linear in each of the arguments $x^1, \ldots, x^r$. Physically, tensors are used to describe linear interactions between physical properties. In the simplest case, scalar properties are modelled by rank zero tensor whereas vector fields (i.e. direction-dependent properties) are modelled by rank-one tensors. An example for a second-rank tensor is the thermal conductivity tensor k_{ij} which describes the linear relationship between the negative temperature gradient $-\text{grad}T = -(\frac{\partial T}{\partial x_1}, \frac{\partial T}{\partial x_2}, \frac{\partial T}{\partial x_3})$, that is a first-order tensor, and the heat flux $q = (q_1, q_2, q_3)$ per unit area which is also a first-order tensor. The linear relationship is given by the equality

$$q_i = - \sum_{j=1}^{3} k_{ij} \frac{\partial T}{\partial x_j}, \quad i = 1, \ldots, 3,$$

and can be seen as a matrix vector product of the thermal conductivity tensor k_{ij} interpreted as a matrix and the negative temperature gradient interpreted as a vector. In the present example the negative temperature gradient is called *applied tensor* and the heat flux is called *induced tensor*.

In the general case, we define a rank r tensor $T_{i_1,...,i_r}$ inductively as the linear relationship between two physical properties which are modelled by a rank s tensor $A_{j_1,j_2,...,j_s}$ and a rank t tensor $B_{k_1,k_2,...,k_t}$, such that the equation $r = t + s$ is satisfied. The rank of a tensor is therefore given by the rank of the induced tensor plus the rank of the applied tensor. The linear dependency between the applied tensor A and the induced tensor B is given by the tensor product

$$B_{k_1,...,k_t} = \sum_{j_1=1}^{3} \sum_{j_1=1}^{3} \cdots \sum_{j_s=1}^{3} T_{k_1,k_2,...,k_t,j_1,...,j_s} A_{j_1,...,j_s}$$

$$= T_{k_1,k_2,...,k_t,j_1,...,j_s} A_{j_1,...,j_s}.$$

In the right-hand side of the last equation we used the Einstein summation convention and omitted the sum sign for every two equal indexes; this will be default in all further formulae.

In MTEX a tensor is represented by a variable of type `tensor`. In order to create such a variable, the r-dimensional matrix has to be specified. As an example we consider the 2nd rank stress tensor σ_{ij}, which can be defined by

```
M = [[1.45 0.00 0.19]; ...
    [0.00 2.11 0.00]; ...
    [0.19 0.00 1.79]];

sigma = tensor (M, 'name', 'stress',
    'unit', 'MPa');

sigma = stress tensor (size: 3 3)
    rank: 2
    unit: MPa

    1.45  0.00  0.19
    0.00  2.11  0.00
    0.19  0.00  1.79
```

Furthermore, we defined the normal $\vec{n} = (1, 0, 0)$ to plane by

```
n = vector3d (1,0,0)
n = vector3d (size: 1 1)
    x  y  z
    1  0  0
```

According to Cauchy's stress principle, the stress vector $T^{\vec{n}}$ associated with the plane normal $\vec{n}$ is then computed by

$$T_j^{\vec{n}} = \sigma_{ij}\, \vec{n}_i\,.$$

In MTEX this equation may be written as

```
T = EinsteinSum (sigma, [-1 1], n, -1,
    'unit', 'MPa')

T = tensor (size: 3)
    unit: MPa
    rank: 1

    1.45
    0
    0.19
```

Note that the -1 in the arguments of the command `EinsteinSum` indicates the dimension which has to be summed up and the 1 in the argument indicates that the second dimension of σ becomes the first dimension of T. Using the stress vector $T^{\vec{n}}$, the scalar magnitudes of the normal stress σ_N and the shear stress σ_S are given as

$$\sigma_N = T_i^{\vec{n}}\, \vec{n}_i = \sigma_{ij}\, \vec{n}_i\, \vec{n}_j \text{ and } \sigma_S = \sqrt{T_i^{\vec{n}} T_i^{\vec{n}} - \sigma_N^2}.$$

In MTEX the corresponding calculation reads as

```
sigmaN = double (EinsteinSum (T, -1, n,
    -1))
sigmaS = sqrt (double(EinsteinSum (T, -1,
    T, -1)) − sigma N^2)
sigmaN = 1.4500
sigmaS = 0.1900
```

The crystal reference frame

Tensors can be classified into two types: matter tensors describing physical properties such as electrical or thermal conductivity, magnetic permeability, etc. of a crystalline specimen, and field tensors describing applied forces such as stress, strain or a electric field to a specimen. Furthermore, it is important to distinguish between single-crystal tensors describing constituent crystal properties and tensors describing averaged macroscopic properties of a polycrystalline specimen. While the reference frame for the latter is the specimen coordinate system, the reference frame for single-crystal tensor properties is unambiguously connected to the crystal coordinate system. The reference frames and their conventions are explained below. We will restrict ourselves to tensors of single or polycrystals defined in a Cartesian reference frame comprising the three unit vectors $\vec{X}^T$, $\vec{Y}^T$, $\vec{Z}^T$. The use of an orthogonal reference frame for single crystals avoids the complications of the metric associated with the crystal unit cell axes. In any case, almost all modern measurements of physical property tensors are reported using Cartesian reference frames.

Table 1. *Alignment of the crystal reference frame for the tensors of physical properties of crystals. The notation $\vec{a}$, $\vec{b}$, $\vec{c}$, $\vec{m}$ corresponds to crystallographic directions in the direct lattice space, whereas the notation $\vec{a}*$, $\vec{b}*$, $\vec{c}*$ denotes the corresponding directions in the reciprocal lattice space, which are parallel to the normal to the plane written as $\perp a$ for $\vec{a}*$, etc. Note that there are at least two possible reference choices for all symmetries except orthorhombic, tetragonal and cubic*

Crystal symmetries	$\vec{X}^T$	$\vec{Y}^T$	$\vec{Z}^T$
Orthorhombic, tetragonal, cubic	$\vec{a}$	$\vec{b}$	$\vec{c}$
Trigonal, hexagonal	$\vec{a}$	$\vec{m}$	$\vec{c}$
	$\vec{m}$	$-\vec{a}$	$\vec{c}$
Monoclinic	$\vec{a}*$	$\vec{b}$	$\vec{c}$
	$\vec{a}$	$\vec{b}$	$\vec{c}*$
Triclinic	$\vec{a}*$	$\vec{Z}^T \times \vec{X}^T$	$\vec{c}$
	$\vec{a}$	$\vec{Z}^T \times \vec{X}^T$	$\vec{c}*$
	$\vec{Y}^T \times \vec{Z}^T$	$\vec{b}*$	$\vec{c}$
	$\vec{Y}^T \times \vec{Z}^T$	$\vec{b}$	$\vec{c}*$

We next discuss how the single-crystal tensor reference frame is defined using the crystal coordinate system. In the general case of triclinic crystal symmetry, the crystal coordinate system is specified by its axis lengths a, b, c and inter-axial angles α, β, γ resulting in a non-Euclidean coordinate system $\vec{a}$, $\vec{b}$, $\vec{c}$ for the general case. In order to align the Euclidean tensor reference frame $\vec{X}^T$, $\vec{Y}^T$, $\vec{Z}^T$ in the crystal coordinate system, several conventions are in use. The most common conventions are summarized in Table 1.

In MTEX the alignment of the crystal reference frame is defined together with the symmetry group and the crystal coordinate system. All this information is stored in a variable of type symmetry. For example by

```
cs_tensor = symmetry('triclinic' [5.29],
    9.18, 9.42],...
    [90.4, 98.9, 90.1]* degree, 'X||a*',
    'Z||c', 'mineral', 'Talc');

cs_tensor = symmetry(size: 1)

mineral : Talc

symmetry : triclinic (−1)
a, b, c : 5.3, 9.2, 9.4
alpha, beta, gamma : 90.4, 98.9, 90.1
reference frame : X||a*, Z||c
```

we store in the variable cs_tensor the geometry of Talc which has triclinic crystal symmetry, axis lengths 5.29, 9.18, 9.42, inter-axial angles 90.4°, 98.9°, 90.1° and the convention for a Cartesian right-handed tensor reference frame $\vec{X}||\vec{a}*$, $\vec{Z}||\vec{c}$;

we therefore have $\vec{Y} = \vec{Z} \times \vec{X}$ for the alignment of the crystal reference frame. In order to define a crystal constituent property tensor with respect to this crystal reference frame, we append the variable cs_tensor to its definition, that is,

```
M = [[219.83 59.66 −4.82 −0.82 −33.87
    −1.04];...
    [59.66 216.38 −3.67 1.79 −16.51
    −0.62];...
    [−4.82 −3.67 48.89 4.12 −15.52
    −3.59];...
    [−0.82 1.79 4.12 26.54 −3.60
    −6.41];...
    [−33.87 −16.51 −15.52 −3.60 22.85
    −1.67];...
    [−1.04 −0.62 −3.59 −6.41 −1.67
    78.29]];

C = tensor(M, 'name', 'elastic stiffness,
    'unit', 'GPa', cs_tensor)

C = elastic stiffness tensor(size : 3 3 3 3)
    unit : GPa
    rank : 4
  mineral : Talc (triclinic, X||a*, Z||c)

tensor in Voigt matrix representation
219.83   59.66  −4.82 −0.82 −33.87 −1.04
 59.66  216.38  −3.67  1.79 −16.51 −0.62
 −4.82   −3.67  48.89  4.12 −15.52 −3.59
 −0.82    1.79   4.12 26.54  −3.60 −6.41
−33.87  −16.51 −15.52 −3.60  22.85 −1.67
 −1.04   −0.62  −3.59 −6.41  −1.67 78.29
```

defines the elastic stiffness tensor in GPa of Talc. This example will be discussed in greater detail in the section 'Elasticity tensors'.

Crystal orientations

Let $\vec{X}^c$, $\vec{Y}^c$, $\vec{Z}^c$ be a Euclidean crystal coordinate system assigned to a specific crystal and let $\vec{X}^s$, $\vec{Y}^s$, $\vec{Z}^s$ be a specimen coordinate system. In polycrystalline materials, the two coordinate systems generally do not coincide. Their relative alignment describes the orientation of the crystal within the specimen. More specifically, the *orientation* of a crystal is defined as the (active) rotation g that rotates the specimen coordinate system into coincidence with the crystal coordinate system. From another point of view, the rotation g can be described as the basis transformation from the crystal coordinate system to the specimen coordinate system. Let $\vec{h} = (h_1, h_2, h_3)$ be the coordinates of a specific direction with respect to the crystal coordinate system. Then $\vec{r} = (r_1, r_2, r_3) = g\vec{h}$ are the coordinates of the same direction with respect to the specimen coordinate system.

Crystal orientations are typically defined by Euler angles, either by specifying rotations with

angles ϕ_1, Φ, ϕ_2 about the axes Z^s, X^s, Z^s (Bunge convention) or with angles α, β, γ about the axes Z^s, Y^s, Z^s (Matthies convention). Both conventions, and also some others, are supported in MTEX. In order to define an orientation in MTEX we start by fixing the crystal reference frame $\vec{X}^c, \vec{Y}^c, \vec{Z}^c$ used for the definition of the orientation,

```
cs_orientation = symmetry('triclinic'
   [5.29], 9.18, 9.42],...
   [90.4, 98.9, 90.1]* degree, 'X||a*',
   'Z||c', 'mineral', 'Talc');

cs_orientation = crystal symmetry
   (size: 1)

mineral : talc
symmetry : triclinic (-1)
a, b, c : 5.3, 9.2, 9.4
alpha, beta, gamma: 90.4, 98.9, 90.1
reference frame : X||a, Z||c*
```

Now an orientation can be defined as a variable of type orientation, it is common practice to use the letter **g** to denote an orientation, derived from the German word *Gefüge* used by Sander (1911).

```
g = orientation ('Euler', 10*degree,
   20*degree, 5*degree, 'Bunge',
   cs_orientation)

g = orientation (size : 1 1)
     mineral : talc
     crystal symmetry : triclinic, X||a,
        Z||c*
     specimen symmetry: triclinic

Bunge Euler angles in degree
phi1 Phi phi2
  10  20    5
```

Note that for the definition of an orientation the crystal reference frame is crucial. The definition of the variable of type orientation therefore includes a variable of type symmetry, storing the relevant information. This applies in particular if the orientation data (i.e. Euler angles) are imported from third-party measurement systems such as EBSD and associated software with their own specific conventions for $\vec{X}^c, \vec{Y}^c, \vec{Z}^c$, which should be defined when using the MTEX import wizard.

In order to demonstrate the coordinate transform between the crystal and the specimen coordinate system, we choose a crystal direction in the reciprocal lattice $\vec{h} = h\,\vec{a}^* + k\vec{b}^* + \ell\vec{c}^*$ (pole to a plane) by defining a variable of type Miller:

```
h = Miller (1, 1, 0, cs_orientation, 'hkl')
h = Miller (size: 1 1)
     mineral : talc (triclinic, X||a,
        Z||c*)
     h  1
     k  1
     l  0
```

and express it in terms of the specimen coordinate system for a specific orientation $g = (10°, 20°, 5°)$

```
r = g * h
r = vector3d (size: 1 1),
     x         y         z
     0.714153 0.62047 0.324041
```

The resulting variable is of type vector3d reflecting that the new coordinate system is the specimen coordinate system. Note that in order that the coordinate transformation rule makes sense physically, the corresponding crystal reference frames used for the definition of the orientation and the crystal direction by Miller indices must coincide. Alternatively, a crystal direction $\vec{u} = u\vec{a} + v\vec{b} + w\vec{c}$ in direct space can be specified:

```
u = Miller (1, 1, 0, cs_orientation, 'uvw')
h = Miller (size: 1 1), uvw
     mineral: talc (triclinic, X||a,
        Z||c*)
     u  1
     v  1
     w  0
```

and expressed in terms of the specimen coordinate system

```
r = g * u
r = vector3d (size: 1 1),
     x         y         z
     0.266258 0.912596 0.310283
```

This obviously gives a different direction, since direct and reciprocal space do not coincide for triclinic crystal symmetry.

The relationship between the single-crystal physical property and Euler angle reference frames

Let us consider a rank r tensor $T_{i_1,...,i_r}$ describing some physical property of a crystal with respect to a well-defined crystal reference frame $\vec{X}^T$, $\vec{Y}^T$, $\vec{Z}^T$. We are often interested in expressing the tensor with respect to another, different Euclidean reference frame $\vec{X}$, $\vec{Y}$, $\vec{Z}$, which might be

(1) a crystallographically equivalent crystal reference frame,
(2) a different convention for aligning the Euclidean reference frame to the crystal coordinate system or
(3) a specimen coordinate system.

Let us first consider a vector $\vec{h}$ that has the representation

$$\vec{h} = h_1^T\,\vec{X}^T + h_2^T\,\vec{Y}^T + h_3^T\,\vec{X}^T$$

with respect to the tensor reference frame $\vec{X}^T$, $\vec{Y}^T$, $\vec{Z}^T$, and the representation

$$\vec{h} = h_1 \vec{X} + h_2 \vec{Y} + h_3 \vec{X}$$

with respect to the other reference frame $\vec{X}$, $\vec{Y}$, $\vec{Z}$. Then the coordinates h_1^T, h_2^T, h_3^T and h_1, h_2, h_3 satisfy the transformation rule

$$\begin{pmatrix} h_1 \\ h_2 \\ h_3 \end{pmatrix} = \underbrace{\begin{pmatrix} \vec{X} \cdot \vec{X}^T & \vec{X} \cdot \vec{Y}^T & \vec{X} \cdot \vec{Z}^T \\ \vec{Y} \cdot \vec{X}^T & \vec{Y} \cdot \vec{Y}^T & \vec{Y} \cdot \vec{Z}^T \\ \vec{Z} \cdot \vec{X}^T & \vec{Z} \cdot \vec{Y}^T & \vec{Z} \cdot \vec{Z}^T \end{pmatrix}}_{=:R} \begin{pmatrix} h_1^T \\ h_2^T \\ h_3^T \end{pmatrix}, \quad (1)$$

that is, the matrix R performs the coordinate transformation from the tensor reference frame $\vec{X}^T$, $\vec{Y}^T$, $\vec{Z}^T$ to the other reference frame $\vec{X}$, $\vec{Y}$, $\vec{Z}$. The matrix R can also be interpreted as the rotation matrix that rotates the second reference frame into coincidence with the tensor reference frame. Considering h_j^T to be a rank-one tensor, the transformation rule becomes

$$h_i = h_j^T R_{ij}.$$

This formula generalizes to arbitrary tensors. Let $T_{i_1,\dots,i_r}^T$ be the coefficients of a rank r tensor with respect to the crystal reference frame X^T, Y^T, Z^T and let $T_{i_1,\dots,i_r}$ be the coefficients with respect to another reference frame X, Y, Z. Then the linear orthogonal transformation law for Cartesian tensors states that

$$T_{i_1,\dots,i_r} = T_{j_1,\dots,j_r}^T R_{i_1 j_1} \cdots R_{i_r j_r}. \quad (2)$$

Let us now examine the three cases for a new reference frame as mentioned at the beginning of this section. In the case of a crystallographically equivalent reference frame, the coordinate transform R is a symmetry element of the crystal and the tensor remains invariant with respect to this coordinate transformation, that is $\tilde{T}_{i_1,\dots,i_r} = T_{i_1,\dots,i_r}$.

In the case that the other reference frame $\vec{X}$, $\vec{Y}$, $\vec{Z}$ follows a different convention in aligning to the crystal coordinate system, the transformed tensor $\tilde{T}_{i_1,\dots,i_r}$ is generally different to the original tensor. In MTEX this change of reference frame is carried out by the command set. Let us consider the elastic stiffness tensor C_{ijkl} of talc (as defined above) as:

```
C = elastic stiffness tensor (size: 3 3 3 3)
    unit: GPa
    rank: 4
```

mineral: talc (triclinic, X||a*, Z||c)

```
219.83  59.66  -4.82 -0.82 -33.87 -1.04
 59.66 216.38  -3.67  1.79 -16.51 -0.62
 -4.82  -3.67  48.89  4.12 -15.52 -3.59
 -0.82   1.79   4.12 26.54  -3.60 -6.41
-33.87 -16.51 -15.52 -3.60  22.85 -1.67
 -1.04  -0.62  -3.59 -6.41  -1.67 78.29
```

and let us consider the reference frame cs_orientation as defined in the previous section

```
cs_orientation = symmetry(Size : 1)
    mineral : talc
    symmetry : triclinic (-1)
    a, b, c : 5.29, 9.18, 9.42
    alpha, beta, gamma: 90.4, 98.9, 90.1
    reference frame : X||a, Z||c*
```

Then the elastic stiffness tensor C_{ijkl} of talc with respect to the reference frame cs_orientation is computed by setting cs_orientation as the new reference frame, that is

```
C_orientation = set(C, 'CS',
  cs_orientation)
C_orientation = elastic stiffness tensor
  (size: 3 3 3 3)
    unit: GPa
    rank: 4
  mineral: talc (triclinic, X||a, Z||c*)

  tensor in Voigt matrix representation
 231.82  63.19  -5.76  0.76  -4.31 -0.59
  63.19 216.31  -7.23  2.85  -5.99 -0.86
  -5.76  -7.23  38.92  2.23 -16.69 -4.3
   0.76   2.85   2.23 25.8   -4.24  1.86
  -4.31  -5.99 -16.69 -4.24  21.9  -0.14
  -0.59  -0.86  -4.3   1.86  -0.14 79.02
```

Finally, we consider the case that the second reference frame is not aligned to the crystal coordinate system but to the specimen coordinate system. According to the previous section, the coordinate transform then defines the orientation g of the crystal and equation (2) tells us how the tensor has to be rotated according to the crystal orientation. In this case we will write

$$\begin{aligned} T_{i_1,\dots,i_r} &= T_{j_1,\dots,j_r}^T(g) \\ &= T_{j_1,\dots,j_r}^T R_{i_1 j_1}(g) \cdots R_{i_r j_r}(g), \quad (3) \end{aligned}$$

to express the dependency of the resulting tensor from the orientation g. Here $R_{i_r j_r}(g)$ is the rotation matrix defined by the orientation g. In order to apply equation (3), it is of major importance that the tensor reference frame and the crystal reference frame used for describing the orientation coincide. If they do not coincide, the tensor has to be transformed to the same crystal reference frame used for describing the orientation. When working

with tensors and orientation data it is therefore always necessary to know the tensor reference frame and the crystal reference frame used for describing the orientation. In practical applications this is not always a simple task, as this information is sometimes hidden by the commercial EBSD systems.

If the corresponding reference frames are specified in the definition of the tensor as well as in the definition of the orientation, MTEX automatically checks for coincidence and performs the necessary coordinate transforms if they do not coincide. Eventually, the rotated tensor for an orientation $g = (10°, 20°, 5°)$ is computed by the command rotate:

```
C_rotated = rotate (C,g)
  C_rotated = elastic_stifness tensor
  (size: 3 3 3 3)
   unit: GPa
   rank: 4

  tensor in Voigt matrix representation
228.79  56.05    1.92 19.99 -13.82   6.85
 56.05 176.08  11.69 50.32   -7.62   4.42
  1.92  11.69  43.27   5.28 -19.48   2.33
 19.99  50.32    5.28 43.41   -1.74   0.24
-13.82  -7.62 -19.48 -1.74  29.35 17.34
  6.85   4.42    2.33  0.24  17.34 73.4
```

Note, that the resulting tensor does not contain any information on the original mineral or reference frame; this is because the single-crystal tensor is now with respect to the specimen coordinate system and can be averaged with any other elastic stiffness tensor from any other crystal of any composition and orientation.

Single-crystal anisotropic properties

We now present some classical properties of single crystals that can be described by tensors (cf. Nye 1985).

Second-rank tensors

A typical second-rank tensor describes the relationship between an applied vector field and an induced vector field, such that the induced effect is equal to the tensor property multiplied by the applied vector. Examples of such a tensor are

- the electrical conductivity tensor, where the applied electric field induces a field of current density,
- the dielectric susceptibility tensor, where the applied electric field intensity induces electric polarization,
- the magnetic susceptibility tensor, where the applied magnetic field induces the intensity of magnetization,

- the magnetic permeability tensor, where the applied magnetic field induces magnetic induction,
- the thermal conductivity tensor, where the applied negative temperature gradient induces heat flux.

As a typical example for a second-rank tensor we consider the thermal conductivity tensor k,

$$k = \begin{pmatrix} k_{11} & k_{12} & k_{13} \\ k_{21} & k_{22} & k_{23} \\ k_{31} & k_{32} & k_{33} \end{pmatrix}$$
$$= \begin{pmatrix} -\dfrac{\partial x_1}{\partial T}q_1 & -\dfrac{\partial x_2}{\partial T}q_1 & -\dfrac{\partial x_2}{\partial T}q_1 \\ -\dfrac{\partial x_1}{\partial T}q_2 & -\dfrac{\partial x_2}{\partial T}q_2 & -\dfrac{\partial x_2}{\partial T}q_2 \\ -\dfrac{\partial x_1}{\partial T}q_3 & -\dfrac{\partial x_2}{\partial T}q_3 & -\dfrac{\partial x_2}{\partial T}q_3 \end{pmatrix}$$

which relates the negative temperature gradient $-\text{grad}\,T = -(\partial T/\partial x_1, \partial T/\partial x_2, \partial T/\partial x_3)$ to the heat flux $q = (q_1, q_2, q_3)$ per unit area by

$$q_i = -\sum_{j=1}^{3} k_{ij}\frac{\partial T}{\partial x_j} = -k_{ij}\frac{\partial T}{\partial x_j}. \qquad (4)$$

In the present example the applied vector is the negative temperature gradient and the induced vector is the heat flux. Furthermore, we see that the relating vector is built up as a matrix where the applied vector is the denominator of the rows and the induced vector is the numerator of columns. We see that the tensor entries k_{ij} describe the heat flux q_i in direction X_i given a thermal gradient $\partial T/\partial x_j$ in direction X_j.

As an example we consider the thermal conductivity of monoclinic orthoclase (Hofer & Schilling 2002). We start by defining the tensor reference frame and the tensor coefficients in W m^{-1} K^{-1}.

```
cs-tensor = symmetry('monoclinic',
  [8.561, 12.996, 7.192],...
  [90, 116.01, 90]*degree, 'mineral',
  'orthoclase','Y||b','Z||c');

M = [[1.45 0.00 0.19];...
   [0.00 2.11 0.00];...
   [0.19 0.00 1.79]];
```

Now the thermal conductivity tensor k is defined by

```
k = tensor (M, 'name', 'thermal_
  conductivity', unit', 'W_1/m_1/K',
  cs_tensor)

k = thermal conductivity tensor (size: 3 3)
    unit : W 1/m 1/K
    rank : 2
    mineral: orthoclase (monoclinic,
      X||a*, Y||b, Z||c)
```
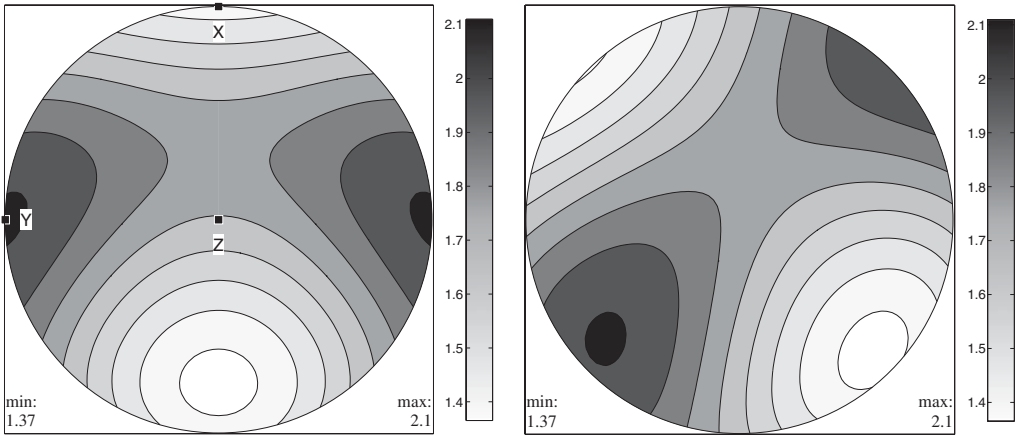
Fig. 1. The thermal conductivity k of orthoclase visualized by its directionally varying magnitude for left: the tensor in standard orientation and right: the rotated tensor.

```
1.45   0      0.19
0      2.11   0
0.19   0      1.79
```

Using the thermal conductivity tensor k we can compute the thermal flux q in W m^{-2} for a temperature gradient in K m^{-1}:

```
gradT = Miller(1,1,0, cs_tensor, 'uvw')
gradT = Miller (size: 1 1), uvw
    mineral: orthoclase (monoclinic,
      X||a*, Y||b, Z||c)
    u  1
    v  1
    w  0
```

by equation (4). In MTEX, this becomes

```
q = EinsteinSum(k, [1 -1],gradT, -1,
    'name', 'thermal_flux', 'unit', 'W_1/
    m^2')

q = thermal flux tensor (size: 3)
    unit : W 1/m^2
    rank : 1
    mineral: orthoclase (monoclinic,
      X||a*, Y||b, Z||c)
     0.672
     1.7606
    -0.3392
```

Note that the -1 in the arguments of the command `EinsteinSum` indicates the dimension which has to be summed up and the 1 in the argument indicates that the first dimension of k becomes the first dimension of q; see equation (4).

A second-order tensor k_{ij} can be visualized by plotting its magnitude $R(\vec{x})$ in a given direction $\vec{x}$,

$$R(\vec{x}) = k_{ij}\,\vec{x}_i\,\vec{x}_j\,.$$

In MTEX the magnitude in a given direction $\vec{x}$ can be computed via

```
x = Miller(1,0,0, cs_tensor, 'uvw');
R = EinsteinSum(k, [-1 -2],x,-1,x,-2)
R = tensor (size:)
    rank : 0
    mineral: orthoclase (monoclinic,
      X||a*, Y||b, Z||c)

    1.3656
```

Again, the negative arguments -1 and -2 indicate which dimensions have to be multiplied and summed up. Alternatively, we can use the command `magnitude`,

```
R = directionalMagnitude (k, x)
```

Since in MTEX the directional magnitude is the default output of the `plot` command, the code

```
plot(k)
colorbar
```

plots the directional magnitude of k with respect to any direction $\vec{x}$ as shown in Figure 1. Note that, by default, the X axis is plotted in the north direction, the Y axis is plotted in the west direction and the Z axis is at the centre of the plot. This default alignment can be changed by the commands `plotx2north`, `plotx2east`, `plotx2south`, `plotx2west`.

When the tensor k is rotated the directional magnitude rotates accordingly. This can be checked in MTEX by

```
g = orientation('Euler',10*degree,
    20*degree,30*degree,cs_tensor);
k_rot = rotate(k,g);
Plot(k_rot)
```

The resulting ploat is shown in Figure 1.

Furthermore, from the directional magnitude we observe that the thermal conductivity tensor k is symmetric, that is, $k_{ij} = k_{ji}$. This implies that the thermal conductivity is an *axial* or *non-polar* property, which means that the magnitude of heat flow is the same in positive or negative crystallographic directions.

We want to emphasize that there are also second-rank tensors which do not describe the relationship between an applied vector field and an induced vector field but relate, for instance, a zero-rank tensor to a second-rank tensor. The thermal expansion tensor α, defined

$$\alpha_{ij} = \frac{\partial \varepsilon_{ij}}{\partial T},$$

is an example of such a tensor which relates a small applied temperature change ∂T (a scalar or zero-rank tensor) to the induced strain tensor ε_{ij} (a second-rank tensor). The corresponding coefficient of volume thermal expansion becomes

$$\frac{1}{V}\frac{\partial V}{\partial T} = \alpha_{ii}.$$

This relationship holds true only for small changes in temperature. For larger changes in temperature, higher-order terms have to be considered (see Fei 1995 for data on minerals). This also applies to other tensors.

Elasticity tensors

We will now present fourth-rank tensors, but restrict ourselves to the elastic tensors. Let σ_{ij} be the second-rank stress tensor and let ε_{kl} be the second-rank infinitesimal strain tensor. Then the fourth-rank elastic stiffness tensor C_{ijkl} describes the stress σ_{ij} induced by the strain ε_{kl}, defined

$$\sigma_{ij} = C_{ijkl}\varepsilon_{kl}, \tag{5}$$

which is known as Hooke's law for linear elasticity. Alternatively, the fourth-order elastic compliance tensor S_{ijkl} describes the strain ε_{kl} induced by the stress σ_{ij}, defined

$$\varepsilon_{kl} = S_{ijkl}\sigma_{ij}.$$

The above definitions may also be written as

$$C_{ijkl} = \frac{\partial \sigma_{ij}}{\partial \varepsilon_{kl}} \quad \text{and} \quad S_{ijkl} = \frac{\partial \varepsilon_{kl}}{\partial \sigma_{ij}}.$$

In the case of static equilibrium for the stress tensor and infinitesimal deformation for the strain

tensor, both tensors are symmetric, that is, $\sigma_{ij} = \sigma_{ji}$ and $\varepsilon_{ij} = \varepsilon_{ji}$. For the elastic stiffness tensor, this implies the symmetry

$$C_{ijkl} = C_{ijlk} = C_{jikl} = C_{jilk}$$

reducing the number of independent entries of the tensor from $3^4 = 81$ to 36. Since the elastic stiffness C_{ijkl} is related to the internal energy U of a body by

$$C_{ijkl} = \frac{\partial}{\partial \varepsilon_{kl}}\left(\frac{\partial U}{\partial \varepsilon_{ij}}\right),$$

assuming constant entropy, we obtain by the Schwarz integrability condition that allows the interchanging of the order of partial derivatives of a function:

$$C_{ijkl} = \frac{\partial}{\partial \varepsilon_{kl}}\left(\frac{\partial U}{\partial \varepsilon_{ij}}\right) = \left(\frac{\partial^2 U}{\partial \varepsilon_{ij}\partial \varepsilon_{kl}}\right) = \left(\frac{\partial^2 U}{\partial \varepsilon_{kl}\partial \varepsilon_{ij}}\right)$$
$$= C_{klij}.$$

Hence,

$$C_{ijkl} = C_{klij}$$

which further reduces the number of independent entries from 36 to 21 (e.g. Mainprice 2007). These 21 independent entries may be efficiently represented in the form of a symmetric 6×6 matrix C_{mn}, $m, n = 1, \ldots, 6$ as introduced by Voigt (1928). The entries C_{mn} of this matrix representation equal the tensor entries C_{ijkl} whenever m and n correspond to ij and kl according to:

m or n	1	2	3	4	5	6
ij or kl	11	22	33	23, 32	13, 31	12, 21

The Voigt notation is used for published compilations of elastic tensors (e.g. Bass 1995; Isaak 2001).

In a similar manner, a Voigt representation S_{mn} is defined for the elastic compliance tensor S_{ijkl}. However, there are additional factors when converting between the Voigt S_{mn} matrix representation and the tensor representation S_{ijkl}. More precisely, for ij, kl, m, n which correspond to each other according to the above table, we have the identities:

$$S_{ijkl}$$
$$= P \cdot S_{mn}, \begin{cases} P = 1, & \text{if both } m, n = 1, 2, 3 \\ P = \frac{1}{2}, & \text{if either } m \text{ or } n \text{ are } 4, 5, 6 \\ P = \frac{1}{4}, & \text{if both } m, n = 4, 5, 6 \end{cases}$$

Using the Voigt matrix representation of the elastic stiffness tensor (equation (5)) may be written as

$$
\begin{pmatrix} \sigma_{11} \\ \sigma_{22} \\ \sigma_{33} \\ \sigma_{23} \\ \sigma_{13} \\ \sigma_{12} \end{pmatrix} = \begin{pmatrix} C_{11} & C_{12} & C_{13} & C_{14} & C_{15} & C_{16} \\ C_{21} & C_{22} & C_{23} & C_{24} & C_{25} & C_{26} \\ C_{31} & C_{32} & C_{33} & C_{34} & C_{35} & C_{36} \\ C_{41} & C_{42} & C_{43} & C_{44} & C_{45} & C_{46} \\ C_{51} & C_{52} & C_{53} & C_{54} & C_{55} & C_{56} \\ C_{61} & C_{62} & C_{63} & C_{64} & C_{65} & C_{66} \end{pmatrix}
$$
$$
\times \begin{pmatrix} \varepsilon_{11} \\ \varepsilon_{22} \\ \varepsilon_{33} \\ 2\varepsilon_{23} \\ 2\varepsilon_{13} \\ 2\varepsilon_{12} \end{pmatrix}.
$$

The matrix representation of Hooke's law allows for a straightforward interpretation of the tensor coefficients C_{ij}. For example the tensor coefficient C_{11} describes the dependency between normal stress σ_{11} in direction X and axial strain ε_{11} in the same direction. The coefficient C_{14} describes the dependency between normal stress σ_{11} in direction X and shear strain $2\varepsilon_{23} = 2\varepsilon_{32}$ in direction Y in the plane normal to Z. The dependency between normal stress σ_{11} and axial strains ε_{11}, ε_{22} and ε_{33} along X, Y and Z is described by C_{11}, C_{12} and C_{13}, whereas the dependencies between the normal stress σ_{11} and shear strains $2\varepsilon_{23}$, $2\varepsilon_{13}$ and $2\varepsilon_{12}$ are described by C_{14}, C_{15} and C_{16}. These effects are most important in low-symmetry crystals, such as triclinic and monoclinic crystals, where there are a large number of non-zero coefficients.

In MTEX the elasticity tensors may be specified directly in Voigt notation as we have already seen in the 'Tensor mathematics and crystal geometry' section. Alternatively, tensors may also be imported from ASCII files using a graphical interface called import wizard in MTEX.

Let C be the elastic stiffness tensor for talc in GPa as defined in 'The crystal reference frame' section.

```
C = elastic_stiffness tensor
   (size: 3 3 3 3)
   unit : GPa
   rank : 4
   mineral: talc (triclinic, X||a*, Z||c)

   tensor in Voigt matrix representation
 219.83   59.66  -4.82 -0.82 -33.87 -1.04
  59.66 -216.38  -3.67  1.79 -16.51 -0.62
  -4.82   -3.67  48.89  4.12 -15.52 -3.59
  -0.82    1.79   4.12 26.54  -3.6  -6.41
 -33.87  -16.51 -15.52 -3.6   22.85 -1.67
  -1.04   -0.62  -3.59 -6.41  -1.67 78.29
```

The elastic compliance S in GPa^{-1} can then be computed by inverting the tensor C.

```
S = inv(C)
S = elastic compliance tensor
   (size: 3 3 3 3)
   unit : 1/GPa
   rank : 4
   mineral: talc (triclinic, X||a*,
      Z||c)

   tensor in Voigt matrix (×10⁻³)
      representation
  6.91  -0.83   4.71  0.74   6.56  0.35
 -0.83   5.14   1.41 -0.04   1.72  0.08
  4.71   1.41  30.31 -0.13  14.35  1.03
  0.74  -0.04  -0.13  9.94   2.12  0.86
  6.56   1.72  14.35  2.12  21.71  1.02
  0.35   0.08   1.03  0.86   1.02  3.31
```

Elastic properties

The fourth-order elastic stiffness tensor C_{ijkl} and fourth-order elastic compliance tensor S_{ijkl} are the starting point for the calculation of a number of elastic anisotropic physical properties, which include

- Young's modulus,
- shear modulus,
- Poisson's ratio,
- linear compressibility,
- compressional and shear elastic wave velocities,
- wavefront velocities,
- mean sound velocities,
- Debye temperature,

and, of course, their isotropic equivalents. In the following we provide a short overview of these properties.

Scalar volume compressibility. First we consider the *scalar volume compressibility β*. Using the fact that the change of volume is given in terms of the strain tensor ε_{ij} by

$$\frac{\partial V}{V} = \varepsilon_{ii},$$

we determine, for hydrostatic or isotropic pressure (which is given by the stress tensor $\sigma_{kl} = -P\delta_{kl}$), that the change of volume is given by

$$\frac{\partial V}{V} = -PS_{iikk}.$$

The volume compressibility is therefore

$$\beta = -\frac{\partial V}{V}\frac{1}{P} = S_{iikk}.$$

Linear compressibility. The *linear compressibility* $\beta(x)$ of a crystal is the strain, that is the relative change in length $\partial l/l$, for a specific crystallographic

direction x when the crystal is subjected to a unit change in hydrostatic pressure $-P\delta_{kl}$. From

$$\frac{\partial l}{l} = \varepsilon_{ij}x_ix_j = -PS_{iikk}x_ix_j$$

we conclude

$$\beta(x) = -\frac{\partial l}{l}\frac{1}{P} = S_{ijkk}x_ix_j.$$

Young's modulus. Young's modulus E is the ratio of the axial (longitudinal) stress to the lateral (transverse) strain in a tensile or compressive test. As we have seen earlier when discussing the elastic stiffness tensor, this type of uniaxial stress is accompanied by lateral and shear strains as well as the axial strain. Young's modulus in direction x is given by

$$E(x) = (S_{ijkl}x_ix_jx_kx_l)^{-1}.$$

Shear modulus. Unlike Young's modulus, the *shear modulus* G in an anisotropic medium is defined using two directions: the shear plane h and the shear direction u. For example, if the shear stress σ_{12} results in the shear strain $2\varepsilon_{12}$ then the corresponding shear modulus is $G = \sigma_{12}/2\varepsilon_{12}$. From Hooke's law we have

$$\varepsilon_{12} = S_{1212}\sigma_{12} + S_{1221}\sigma_{21},$$

and hence $G = (4S_{1212})^{-1}$. The shear modulus for an arbitrary, but orthogonal, shear plane h and shear direction u is given by

$$G(h, u) = (4S_{ijkl}h_iu_jh_ku_l)^{-1}.$$

Poisson ratio. The anisotropic *Poisson ratio* is defined by the elastic strain in two orthogonal directions: the longitudinal (or axial) direction x and the transverse (or lateral) direction y. The lateral strain is defined by $-\varepsilon_{ij}y_iy_j$ along y and the longitudinal strain by $\varepsilon_{ij}x_ix_j$ along x. The anisotropic Poisson ratio $\nu(x, y)$ is given as the ratio of lateral to longitudinal strain (Sirotin & Shakolskaya 1982) as

$$\nu(x, y) = -\frac{\varepsilon_{ij}y_iy_j}{\varepsilon_{kl}x_kx_l} = -\frac{S_{ijkl}x_ix_jy_ky_l}{S_{mnop}x_mx_nx_ox_p}.$$

The anisotropic Poisson ratio has recently been reported for talc (Mainprice *et al.* 2008) and has been found to be negative for many directions at low pressure.

Wave velocities. The Christoffel equation, first published by Christoffel (1877), can be used to calculate elastic wave velocities and the polarizations in an anisotropic elastic medium from the elastic stiffness tensor C_{ijkl} or, more straightforward, from the Christoffel tensor T_{ik} which is, for a unit propagation direction $\vec{n}$, defined by

$$T_{ik}(\vec{n}) = C_{ijkl}\,\vec{n}_j\,\vec{n}_l\,.$$

Since the elastic tensors are symmetric, we have

$$T_{ik}(\vec{n}) = C_{ijkl}n_jn_l = C_{jikl}\,\vec{n}_j\,\vec{n}_l = C_{ijlk}\,\vec{n}_j\,\vec{n}_l$$
$$= C_{klij}\,\vec{n}_j\,\vec{n}_l = T_{ki}(\vec{n}),$$

and hence the Christoffel tensor $T(\vec{n})$ is symmetric. The Christoffel tensor is also invariant upon the change of sign of the propagation direction, as the elastic tensor is not sensitive to the presence or absence of a centre of crystal symmetry (being a centro-symmetric physical property).

Because the elastic strain energy $1/2C_{ijkl}\,\varepsilon_{ij}\varepsilon_{kl}$ of a stable crystal is always positive and real (e.g. Nye 1985), the eigenvalues λ_1, λ_1 and λ_3 of the Christoffel tensor $T_{ik}(\vec{n})$ are real and positive. They are related to the wave velocities V_p, V_{s1} and V_{s2} of the plane P-, S1- and S2-waves propagating in the direction $\vec{n}$ by the formulae

$$V_p = \sqrt{\frac{\lambda_1}{\rho}}, \quad V_{s1} = \sqrt{\frac{\lambda_2}{\rho}}, \quad V_{s2} = \sqrt{\frac{\lambda_3}{\rho}},$$

where ρ denotes the material density. The three eigenvectors of the Christoffel tensor are the polarization directions, also called vibration, particle movement or displacement vectors, of the three waves. As the Christoffel tensor is symmetric, the three polarization directions are mutually perpendicular. In the most general case there are no particular angular relationships between polarization directions p and the propagation direction $\vec{n}$. However, the P-wave polarization direction is typically nearly parallel and the two S-waves polarizations are nearly perpendicular to the propagation direction. They are termed quasi-P or quasi-S waves. The S-wave velocities may be identified unambiguously by their relative velocity $V_{s1} > V_{s2}$.

All the elastic properties mentioned in this section have direct expressions in MTEX:

```
beta = volumeCompressibility (C)
beta = linearCompressibility (C,x)
   E = YoungsModulus (C,x)
   G = shearModulus (C,h,u)
  nu = PoissonRatio (C,x,y)
   T = ChristoffelTensor (C,n)
```
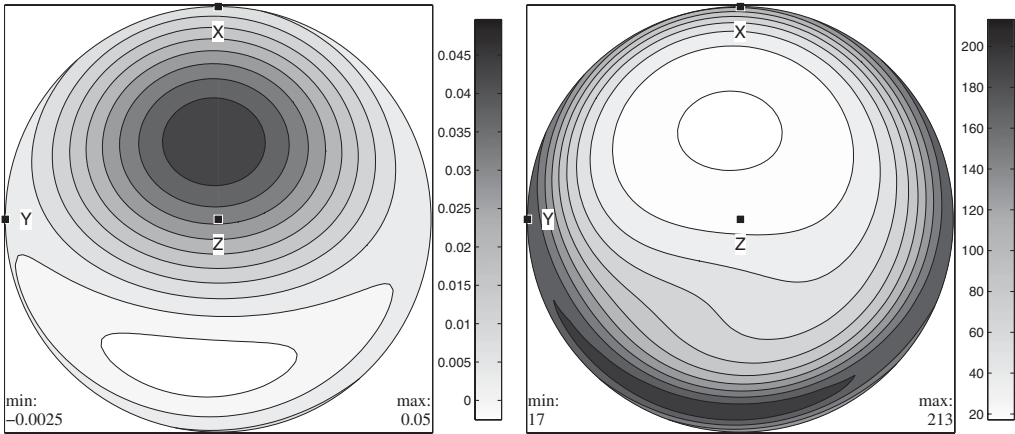
Fig. 2. Left: the linear compressibility in GPa^{-1} and right: Young's modulus in GPa for talc.

Note that all these commands take the compliance tensor C as basis for the calculations. For the calculation of the wave velocities the command velocity

```
[vp, vs1, vs2, pp, ps1, ps2] = velocity
(C,x ,rho)
```

allows for the computation of the wave velocities and the corresponding polarization directions.

Visualization

In order to visualize the above quantities, MTEX offers a simple, yet flexible, syntax. Let us demonstrate it using the Talc example of the previous section. In order to plot the linear compressibility $\beta(\vec{x})$ or Young's Modulus $E(\vec{x})$ as a function of the direction $\vec{x}$, we use the commands

```
plot (C, 'PlotType',
   'linearCompressibility')
plot (C, 'PlotType', 'YoungsModulus')
```

The resulting plots are shown in Figure 2.

Next we want to visualize the wave velocities and the polarization directions. Let us start with the P-wave velocity in km s^{-1} which is plotted by

```
rho = 2.78276;
plot (C, 'PlotType', 'velocity', 'vp',
   'density', rho)
```

Note that we had to pass the density rho in g cm^{-3} to the plot command. We now want to plot the P-wave polarization directions on top, so use the commands

hold on and hold off to prevent MTEX from clearing the output window:

```
hold on
plot(C, 'PlotType', 'velocity', 'pp',
   'density', rho);
hold off
```

The result is shown in Figure 3. Instead of only specifying the variables to plot, we can also perform simple calculations. From the commands

```
plot (C, 'PlotType', 'velocity',
   '200*(vs1-vs2)./(vs1+vs2)',
   'density', rho);
hold on
plot (C, 'PlotType', 'velocity', 'ps1',
   'density', rho);
hold off
```

the S-wave anisotropy in percent is plotted together with the polarization directions of the fastest S-wave ps1. Another example illustrating the flexibility of the system is the following plot of the velocity ratio V_p/V_{s1} together with the direction of the S1-wave polarizations.

```
plot (C, 'PlotType', 'velocity',
   'vp./vs1', 'density', rho);
hold on
plot (C, 'PlotType', 'velocity','ps1',
   'density', rho);
hold off
```

Anisotropic properties of polyphase aggregates

In this section we are concerned with the problem of calculating average physical properties of
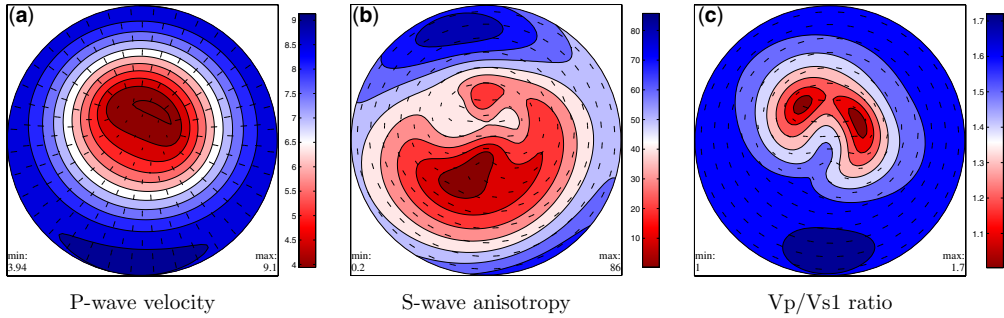
Fig. 3. Wave velocities of a Talc crystal plotted on seismic colour maps: (**a**) P-wave velocity together with the P-wave polarization direction; (**b**) S-wave anisotropy in percent together with the S1-wave polarization direction; and (**c**) the ratio of Vp/Vs1 velocities together with the S1-wave polarization direction.

polyphase aggregates. To this end, two ingredients are required for each phase p:

(1) the property tensor $T^p_{i_1,\dots,i_r}$ describing the physical behaviour of a single crystal in the reference orientation,

(2) the *orientation density function* (ODF) $f^p(g)$ describing the volume portion $\Delta V/V$ of crystals having orientation g or a representative set of individual orientations g_m, $m = 1, \dots, M$ (e.g. measured by EBSD).

As an example we consider an aggregate composed of two minerals (glaucophane and epidote) using data from a blueschist from the Ile de Groix, France. The corresponding crystal reference frames are defined by

```
cs_glaucophane = symmetry ('2/m',
   [9.5334, 17.7347, 5.3008],[90.00,
   103.597, 90.00] * degree, 'mineral',
   'glaucophane');

cs_epidote = symmetry ('2/m', [8.8877,
   5.6275, 10.1517],[90.00, 115.383,
   90.00] * degree, 'mineral',
   'epidote');
```

For glaucophane the elastic stiffness was measured by Bezacier *et al.* (2010) who provided the tensor

```
C_glaucophane = tensor (size: 3 3 3 3)
     rank : 4
  mineral: glaucophane (2/m, X||a*,
     Y||b, Z||c)

  tensor in Voigt matrix representation
122.28  45.69  37.24  0      2.35   0
 45.69 231.5   74.91  0     -4.78   0
 37.24  74.91 254.57  0    -23.74   0
  0      0      0     79.67  0      8.89
  2.35  -4.78 -23.74  0     52.82   0
  0      0      0      8.89  0     51.24
```

For epidote, the elastic stiffness was measured by Aleksandrov *et al.* (1974):

```
C_epidote = tensor (size: 3 3 3 3)
     rank : 4
   mineral: epidote (2/m, X||a*, Y||b,
     Z||c)

   tensor in Voigt matrix
     representation
211.5  65.6   43.2   0    -6.5   0
 65.6 239     43.6   0   -10.4   0
 43.2  43.6  202.1   0   -20     0
  0      0      0    39.1  0    -2.3
 -6.5 -10.4  -20     0    43.4   0
  0      0      0    -2.3  0    79.5
```

Computing the average tensor from individual orientations

We start with the case that we have individual orientation data g_m, $m = 1, \dots, M$, that is, from EBSD or U-stage measurements, and volume fractions V_m, $m = 1, \dots, M$. The best-known averaging techniques for obtaining estimates of the effective properties of aggregates are those developed for elastic constants by Voigt (1887, 1928) and Reuss (1929). The *Voigt average* is defined by assuming that the induced tensor (in broadest sense, including vectors) field is everywhere homogeneous or constant, that is, the induced tensor at every position is set equal to the macroscopic induced tensor of the specimen. In the classical example of elasticity, the strain field is considered constant. The Voigt average is sometimes called the 'series' average by analogy with Ohm's law for electrical circuits.

The Voigt average specimen effective tensor $\langle T \rangle^{\text{Voigt}}$ is defined by the volume average of the individual tensors $T(g^c_m)$ with crystal orientations g^c_m and volume fractions V_m:

$$\langle T \rangle^{\text{Voigt}} = \sum_{m=1}^{M} V_m T(g^c_m).$$

Contrarily, the *Reuss average* is defined by assuming that the applied tensor field is everywhere constant, that is, the applied tensor at every position is set equal to the macroscopic applied tensor of the specimen. In the classical example of elasticity, the stress field is considered constant. The Reuss average is sometimes called the 'parallel' average. The specimen effective tensor $\langle T \rangle^{\text{Reuss}}$ is defined by the volume ensemble average of the inverses of the individual tensors $T^{-1}(g_m^c)$:

$$\langle T \rangle^{\text{Reuss}} = \left[\sum_{m=1}^{M} V_m T^{-1}(g_m^c) \right]^{-1}.$$

The experimentally measured tensor of aggregates is generally between the Voigt and Reuss average bounds as the applied and induced tensor fields distributions are expected to be between uniform induced (Voigt bound) and uniform applied (Reuss bound) field limits. Hill (1952) observed that the arithmetic mean of the Voigt and Reuss bounds

$$\langle T \rangle^{\text{Hill}} = \tfrac{1}{2}(\langle T \rangle^{\text{Voigt}} + \langle T \rangle^{\text{Reuss}}),$$

sometimes called the Hill or Voigt–Reuss–Hill (VRH) average, is often close to experimental values for the elastic fourth-order tensor. Although the VRH average has no theoretical justification, it is widely used in earth and materials sciences.

In the example outlined above of an aggregate consisting of glaucophane and epidote, we consider an EBSD dataset measured by Bezacier *et al.* (2010). In MTEX such individual orientation data are represented by a variable of type EBSD which is generated from an ASCII file containing the individual orientation measurements by the command:

```
ebsd = loadEBSD ('FileName',
       {cs_glaucophane, cs_epidote})
ebsd = EBSD (Groix_A50_5_stitched. ctf)

    properties: bands, bc, bs, error, mad
    phase orientations mineral symmetry
       crystal reference frame
       1 055504 glaucophane 2/m X||a*,
          Y||b, Z||c
       2 63694 epidote 2/m X||a*, Y||b,
          Z||c
```

It should be noted that for both minerals the crystal reference frames have to be specified in the command loadEBSD.

The Voigt, Reuss and Hill average tensors can now be computed for each phase separately by the command calcTensor:

```
[TVoigt, TReuss, THill] = calcTensor
   (ebsd, C_epidote, 'phase', 2)
```

```
C_Voigt = tensor (size: 3 3 3 3)
   rank: 4

   tensor in Voigt matrix representation
   215     55.39  66.15 -0.42  3.02 -4.69
    55.39 179.04  59.12  1.04 -1.06  0.06
    66.15  59.12 202.05  0.94  1.16 -0.77
    -0.42   1.04   0.94 60.67 -0.86 -0.55
     3.02  -1.06   1.16 -0.86 71.77 -0.65
    -4.69   0.06  -0.77 -0.55 -0.65 57.81

C_Reuss = tensor (size: 3 3 3 3)
   rank: 4

   tensor in Voigt matrix representation
   201.17  56.48  65.94 -0.28  3.21 -4.68
    56.48 163.39  61.49  1.23 -1.58 -0.13
    65.94  61.49 189.67  1.29  0.75 -0.64
    -0.28   1.23   1.29 52.85 -0.99 -0.38
     3.21  -1.58   0.75 -099 65.28 -0.6
    -4.68  -0.13  -0.64 -0.38 -0.6  50.6

   C_Hill = tensor (size: 3 3 3 3)
   rank: 4

   tensor in Voigt matrix representation
   208.09  55.93  66.05 -0.35  3.11 -4.69
    55.93 171.22  60.31  1.13 -1.32 -0.04
    66.05  60.31 195.86  1.11  0.96 -0.71
    -0.35   1.13   1.11 56.76 -0.93 -0.46
     3.11  -1.32   0.96 -0.93 68.52 -0.62
    -4.69  -0.04  -0.71 -0.46 -0.62 54.21
```

If no phase is specified and all the tensors for all phases are specified, the command

```
[TVoigt, TReuss, THill] = calcTensor
   (ebsd, C_glaucophane, C_epidote)
```

computes the average over all phases. These calculations have been validated using the Careware FORTRAN code (Mainprice 1990). We emphasize that MTEX automatically checks for the agreement of the EBSD and tensor reference frames for all phases. In case different conventions have been used, MTEX automatically transforms the EBSD data into the convention of the tensors.

Computing the average tensor from an ODF

Next we consider the case that the texture is given by an ODF *f*. The ODF may originate from texture modelling (Bachmann *et al.* 2010), pole figure inversion (Hielscher & Schaeben 2008) or density estimation from EBSD data (Hielscher *et al.* 2010). All these diverse sources may be handled by MTEX.

Given an ODF *f*, the Voigt average $\langle T \rangle^{\text{Voigt}}$ of a tensor *T* is defined by the integral

$$\langle T \rangle^{\text{Voigt}} = \int_{\text{SO(3)}} T(g)f(g)\mathrm{d}g \qquad (6)$$

whereas the Reuss average $\langle T \rangle^{\text{Reuss}}$ is defined as

$$\langle T \rangle^{\text{Reuss}} = \left[\int_{\text{SO(3)}} T^{-1}(g)f(g)\mathrm{d}g \right]^{-1}. \quad (7)$$

Equations (6) and (7) can be computed in two different ways. First, we can use a quadrature rule: for a set of orientations g_m and weights ω_m, the Voigt average is approximated by

$$\langle T \rangle^{\text{Voigt}} \approx \sum_{m=1}^{M} T(g_m)\omega_m f(g_m).$$

Clearly, the accuracy of the approximation depends on the number of nodes g_m and the smoothness of the ODF. An alternative approach to compute the average tensor, avoiding this dependency, uses the expansion of the rotated tensor into generalized spherical harmonics, $D_{kk'}^{\ell}(g)$. Let $T_{i_1,\ldots,i_r}$ be a tensor of rank r. It is well known (cf. Kneer 1965; Bunge 1968; Ganster & Geiss 1985; Humbert & Diz 1991; Mainprice & Humbert 1994; Morris 2006) that the rotated tensor $T_{i_1,\ldots,i_r}(g)$ has an expansion into generalized spherical harmonics up to order r,

$$T_{i_1,\ldots,i_r}(g) = \sum_{\ell=0}^{r} \sum_{k,k'=-\ell}^{\ell} \hat{T}_{i_1,\ldots,i_r}(l, k, k')D_{kk'}^{\ell}(g). \quad (8)$$

The explicit calculations of the coefficients $\hat{T}_{i_1,\ldots,i_r}(l, k, k')$ are given in the Appendix. Assume that the ODF has an expansion into generalized spherical harmonics of the form

$$f(g) = \sum_{\ell=0}^{r} \sum_{k,k'=-\ell}^{\ell} \hat{f}(l, k, k')D_{kk'}^{\ell}(g).$$

The average tensor with respect to this ODF can then be computed by the formula

$$\frac{1}{8\pi^2} \int_{\text{SO(3)}} T_{i_1,\ldots,i_r}(g)f(g)$$

$$= \frac{1}{8\pi^2} \int_{\text{SO(3)}} T_{i_1,\ldots,i_r}(g)\overline{f(g)}dg$$

$$= \sum_{\ell=0}^{r} \frac{1}{2\ell+1} \sum_{k,k'=-\ell}^{\ell} \hat{T}_{i_1,\ldots,i_r}(l, k, k')\overline{\hat{f}(l, k, k')}.$$

By default MTEX uses the Fourier approach, which is much faster than using numerical integration (quadrature rule) which requires a discretization of the ODF. Numerical integration is applied only in the cases when MTEX cannot

determine the Fourier coefficients of the ODF in an efficient manner. At the present time, only the Bingham distributed ODFs pose this problem. All the necessary calculations are done automatically, including the correction for different crystal reference frames.

Let us consider once again the aggregate consisting of glaucophane and epidote and the corresponding EBSD dataset as mentioned in the first section. For any phase, we can then estimate an ODF by

```
odf_epidote = calcODF (ebsd, 'phase', 2)
odf_epidote = ODF (ODF estimated from
  Groix_A50_5 _stitched. ctf)
    mineral : epidote
    crystal symmetry : 2/m, X||a*, Y||b,
      Z||c
    specimen symmetry: triclinic

    Portion specified by Fourier
      coefficients:
      degree: 28
      weight: 1
```

Next, we can compute the average tensors directly from the ODF

```
[TVoigt, TReuss, THill] = calcTensor
(odf_epidote, C_epidote)
C_Voigt = tensor (size: 3 3 3)
  rank: 4

  tensor in Voigt matrix representation
  212.64  56.81  65.68 -0.25  2.56 -4
   56.81 179.21  59.64  0.93 -0.83 -0.27
   65.68  59.64 201.3   0.87  1.12 -0.71
   -0.25   0.93   0.87 61.33 -0.79 -0.35
    2.56  -0.83   1.12 -0.79 71.1  -0.48
   -4      -0.27  -0.71 -0.35 -0.48 59.29

C_Reuss = tensor (size: 3 3 3)
  rank: 4

  tensor in Voigt matrix representation
  197.91  57.92  65.4  -0.09  2.53 -4
   57.92 163.68  61.84  1.13 -1.27 -0.4
   65.4   61.84 188.53  1.21  0.7  -0.58
   -0.09   1.13   1.21 53.39 -0.9  -0.26
    2.53  -1.27   0.7  -0.9  64.34 -0.42
   -4      -0.4   -0.58 -0.26 -0.42 51.7

C_Hill = tensor (size: 3 3 3)
  rank: 4

  tensor in Voigt matrix representation
  205.28  57.36  65.54 -0.17  2.54 -4
   57.36 171.45  60.74  1.03 -1.05 -0.33
   65.54  60.74 194.92  1.04  0.91 -0.64
   -0.17   1.03   1.04 57.36 -0.84 -0.31
    2.54  -1.05   0.91 -0.84 67.72 -0.45
   -4      -0.33  -0.64 -0.31 -0.45 55.49
```

Note that there is a difference between the average tensors calculated directly from the EBSD data and the average tensors calculated from the

estimated ODF. These differences result from the smoothing effect of the kernel density estimation (cf. van den Boogaart 2001). The magnitude of the difference depends on the actual choice of the kernel. It is smaller for sharper kernels, or more precisely for kernels with leading Fourier coefficients close to1. An example for a family of well-suited kernels can be found in Hielscher (2010).

Conclusions

An extensive set of functions have been developed and validated for the calculation of anisotropic crystal physical properties using Cartesian tensors for the MTEX open-source MatLab toolbox. The functions can be applied to tensors of single or polycrystalline materials. The average tensors of polycrystalline and multi-phase aggregates using the Voigt, Reuss and Hill methods have been implemented using three methods: (a) the weighted summation for individual orientation data (e.g. EBSD); (b) the weighted integral of the ODF; and (c) using the Fourier coefficients of the ODF. Special attention has been paid to the crystallographic reference frame used for orientation data (e.g. Euler angles) and Cartesian tensors, as these reference frames are often different in low-symmetry crystals and dependent on the provenance of the orientation and tensor data. The suite of MTEX functions can be used to construct project-specific MatLab M-files and to process orientation data of any type in a coherent workflow from the texture analysis to the anisotropic physical properties. A wide range of graphical tools provides publication quality output in a number of formats. The construction of M-files for specific problems provides a problem-solving method for teaching elementary to advanced texture analysis and anisotropic physical properties. The open-source nature of this project (http://mtex.googlecode.com) allows researchers to access all the details of their calculations, check intermediate results and further the project by adding new functions on Linux, Mac OSX or Windows platforms.

Appendix: Fourier coefficients of the rotated tensor

In this section we are concerned with the Fourier coefficients of tensors, since they are required in equation (8). Previous work on this problem can be found in Jones (1985). Here we present explicit formulae for the Fourier coefficients $\hat{T}_{m_1,\dots,m_r}(J, L, K)$ in terms of the tensor coefficients $T_{m_1,\dots,m_r}(g)$. In particular, we show that the order of the Fourier expansion is bound by the rank of the tensor.

Let us first consider the case of a rank-one tensor T_m. Given an orientation $g \in SO(3)$, the rotated tensor may be expressed as

$$T_m(g) = T_n R_{mn}(g)$$

where $R_{ij}(g)$ is the rotation matrix corresponding to the orientation g. Since the entries of the rotation matrix $R(g)$ are related to the generalized spherical harmonics $D^1_{\ell k}(g)$ by

$$R_{mn}(g) = D^1_{\ell k} U_{m\ell} \overline{U_{nk}},$$

$$U = \begin{pmatrix} \frac{1}{\sqrt{2}}i & 0 & -\frac{1}{\sqrt{2}}i \\ -\frac{1}{\sqrt{2}}i & 0 & \frac{1}{\sqrt{2}}i \\ 0 & i & 0 \end{pmatrix},$$

we obtain

$$T_m(g) = T_n D^1_{\ell k} U_{m\ell} \overline{U_{nk}}.$$

The Fourier coefficients $\hat{T}_m(1, \ell, k)$ of $T_m(g)$ are therefore given by

$$\hat{T}_m(1, \ell, k) = T_n U_{m\ell} \overline{U_{nk}}.$$

Next we switch to the case of a rank-two tensor $T_{m_1 m_2}(g)$. In this case we obtain

$$
\begin{aligned}
&T_{m_1 m_2}(g) \\
&= T_{n_1 n_2} R_{m_1 n_1}(g) R_{m_2 n_2}(g) \\
&= T_{n_1 n_2} D^1_{\ell_1 k_1}(g) U_{m_1 \ell_1} \overline{U_{n_1 k_1}} D^1_{\ell_2 k_2}(g) U_{m_2 \ell_2} \overline{U_{n_2 k_2}}.
\end{aligned}
$$

With the Clebsch Gordan coefficients $\langle j_1 m_1 j_2 m_2 | JM \rangle$ (cf. Varshalovich *et al.* 1988), we have

$$
D_{\ell_1 k_1}^{j_1}(g) D_{\ell_2 k_2}^{j_2}(g)
$$
$$
= \sum_{J=0}^{j_1+j_2} \langle j_1 \ell_1 j_2 \ell_2 | JL \rangle \langle j_1 k_1 j_2 k_2 | JK \rangle D_{LK}^{J}(g) \tag{9}
$$

and hence

$$
T_{m_1 m_2}(g) = \sum_{J=0}^{2} T_{n_1 n_2} U_{m_1 \ell_1} \overline{U_{n_1 k_1}} U_{m_2 \ell_2} \overline{U_{n_2 k_2}}
$$
$$
\langle 1\ell_1 1\ell_2 | JL \rangle \langle 1k_1 1k_2 | JK \rangle D_{LK}^{J}(g).
$$

Finally, for the Fourier coefficients of $T_{mm'}$, we obtain

$$
\hat{T}_{m_1 m_2}(J,L,K) = T_{n_1 n_2} U_{m_1 \ell_1} \overline{U_{n_1 k_1}} U_{m_2 \ell_2} \overline{U_{n_2 k_2}}
$$
$$
\langle 1\ell_1 1\ell_2 | JL \rangle \langle 1k_1 1k_2 | JK \rangle.
$$

For a third-rank tensor we have

$$
T_{m_1 m_2 m_3}(g) = T_{n_1 n_2 n_3} R_{m_1 n_1}(g) R_{m_2 n_2}(g) R_{m_3 n_3}(g)
$$
$$
= T_{n_1 n_2 n_3} D_{\ell_1 k_1}^{1} U_{m_1 \ell_1} \overline{U_{n_1 k_1}} D_{\ell_2 k_2}^{1}
$$
$$
U_{m_2 \ell_2} \overline{U_{n_1 k_2}} D_{\ell_3 k_3}^{1} U_{m_3 \ell_3} \overline{U_{n_1 k_3}}.
$$

Using equation (9) we obtain

$$
T_{m_1 m_2 m_3}(g)
$$
$$
= T_{n_1 n_2 n_3} D_{\ell_1 k_1}^{1} U_{m_1 \ell_1} \overline{U_{n_1 k_1}} D_{\ell_2 k_2}^{1} U_{m_2 \ell_2} \overline{U_{n_1 k_2}} D_{\ell_3 k_3}^{1}
$$
$$
U_{m_3 \ell_3} \overline{U_{n_1 k_3}}
$$
$$
= \sum_{J_1=0}^{2} T_{n_1 n_2 n_3} U_{m_1 \ell_1} \overline{U_{n_1 k_1}} U_{m_2 \ell_2} \overline{U_{n_1 k_2}} U_{m_3 \ell_3} \overline{U_{n_1 k_3}}
$$
$$
\langle 1\ell_1 1\ell_2 | J_1 L_1 \rangle \langle 1k_1 1k_2 | J_1 K_1 \rangle D_{L_1 K_1}^{J_1}(g) D_{\ell_3 k_3}^{1}
$$
$$
= \sum_{J_1=0}^{2} \sum_{J_2=0}^{J_1+1} T_{n_1 n_2 n_3} U_{m_1 \ell_1} \overline{U_{n_1 k_1}} U_{m_2 \ell_2} \overline{U_{n_1 k_2}} U_{m_3 \ell_3} \overline{U_{n_1 k_3}}
$$
$$
\langle 1\ell_1 1\ell_2 | J_1 L_1 \rangle \langle 1k_1 1k_2 | J_1 K_1 \rangle
$$
$$
\langle J_1 L_1 1\ell_3 | J_2 L_2 \rangle \langle J_1 K_1 1k_3 | J_2 K_2 \rangle D_{L_2 K_2}^{J_2}(g).
$$

The coefficients of $T_{m_1 m_2 m_3}$ are therefore given by

$$
\hat{T}_{m_1 m_2 m_3}(J_2, L_2, K_2)
$$
$$
= \sum_{J_1=J_2-1}^{2} T_{n_1 n_2 n_3} U_{m_1 \ell_1} \overline{U_{n_1 k_1}} U_{m_2 \ell_2} \overline{U_{n_1 k_2}} U_{m_3 \ell_3} \overline{U_{n_1 k_3}}
$$
$$
\langle 1\ell_1 1\ell_2 | J_1 L_1 \rangle \langle 1k_1 1k_2 | J_1 K_1 \rangle
$$
$$
\langle J_1 L_1 1\ell_3 | J_2 L_2 \rangle \langle J_1 K_1 1k_3 | J_2 K_2 \rangle.
$$

Finally, we consider the case of a fourth-rank tensor T_{m_1,m_2,m_3,m_4}. Here we have

$$
T_{m_1,m_2,m_3,m_4}
$$
$$
= T_{n_1,n_2,n_3,n_4} D_{m_1,n_1}^{1} D_{m_2,n_2}^{1} D_{m_3,n_3}^{1} D_{m_4,n_4}^{1}
$$
$$
= T_{n_1,n_2,n_3,n_4} \sum_{J_1=0}^{2} \sum_{J_2=0}^{2} \langle 1m_1 1m_2 | J_1 M_1 \rangle \langle 1n_1 1n_2 | J_1 N_1 \rangle
$$
$$
D_{M_1,N_1}^{J_1} \langle 1m_3 1m_4 | J_2 M_2 \rangle \langle 1n_3 1n_4 | J_2 N_2 \rangle D_{M_2,N_2}^{J_2}
$$
$$
= T_{n_1,n_2,n_3,n_4} \sum_{J_0=0}^{4} \sum_{J_1=0}^{2} \sum_{J_2=0}^{2} \langle 1m_1 1m_2 | J_1 M_1 \rangle
$$
$$
\langle 1n_1 1n_2 | J_1 N_1 \rangle \langle 1m_3 1m_4 | J_2 M_2 \rangle \langle 1n_3 1n_4 | J_2 N_2 \rangle
$$
$$
\langle J_1 M_1 J_2 M_2 | J_0 M_0 \rangle \langle J_1 N_1 J_2 N_2 | J_0 N_0 \rangle D_{M_0,N_0}^{J_0}
$$

and hence

$$
\hat{T}_{m_1,m_2,m_3,m_4}(J_0, M_0, N_0)
$$
$$
= \sum_{J_1=0}^{2} \sum_{J_2=0}^{2} \langle 1m_1 1m_2 | J_1 M_1 \rangle \langle 1n_1 1n_2 | J_1 N_1 \rangle
$$
$$
\langle 1m_3 1m_4 | J_2 M_2 \rangle \langle 1n_3 1n_4 | J_2 N_2 \rangle
$$
$$
\langle J_1 M_1 J_2 M_2 | J_0 M_0 \rangle \langle J_1 N_1 J_2 N_2 | J_0 N_0 \rangle.
$$

References

ALEKSANDROV, K. S., ALCHIKOV, U. V., BELIKOV, B. P., ZASLAVSKII, B. I. & KRUPNYI, A. I. 1974. Velocities of elastic waves in minerals at atmospheric pressure and increasing precision of elastic constants by means of EVM (in Russian). *Izvestiya of the Academy of the Sciences of the USSR, Geologic Series*, **10**, 15–24.

BACHMANN, F., HIELSCHER, H., JUPP, P. E., PANTLEON, W., SCHAEBEN, H. & WEGERT, E. 2010. Inferential statistics of electron backscatter diffraction data from within individual crystalline grains. *Journal of Applied Crystallography*, **43**, 1338–1355.

BASS, J. D. 1995. Elastic properties of minerals, melts, and glasses. *In*: AHRENS, T. J. (ed.) *Handbook of Physical Constants*. American Geophysical Union, Special Publication, 45–63.

BEZACIER, L., REYNARD, B., BASS, J. D., WANG, J. & MAINPRICE, D. 2010. Elasticity of glaucophane and seismic properties of high-pressure low-temperature oceanic rocks in subduction zones. *Tectonophysics*, **494**, 201–210.

BUNGE, H.-J. 1968. Über die elastischen konstanten kubischer materialien mit beliebiger textur. *Kristall und Technik*, **3**, 431–438.

CASEY, M. 1981. Numerical analysis of x-ray texture data: an implementation in FORTRAN allowing triclinic or axial specimen symmetry and most crystal symmetries. *Tectonophysics*, **78**, 51–64.

CHRISTOFFEL, E. B. 1877. Über die Fortpflanzung van Stössen durch elastische feste Körper. *Annali di Matematica pura ed applicata, Serie II*, **8**, 193–243.

FEI, Y. 1995. Thermal expansion. *In*: AHRENS, T. J. (ed.) *Minerals Physics and Crystallography: A Handbook of Physical Constants*. American Geophysical Union, Washington, DC, 29–44.

GANSTER, J. & GEISS, D. 1985. Polycrystalline simple average of mechanical properties in the general (triclinic) case. *Physica Status Solidi (B)*, **132**, 395–407.

HIELSCHER, R. 2010. Kernel density estimation on the rotation group, Preprint, Fakultät für Mathematik, TU Chemnitz. http://www.tu-chemnitz.de/mathematik/preprint/2010/PREPRINT_07.php.

HIELSCHER, R. & SCHAEBEN, H. 2008. A novel pole figure inversion method: specification of the MTEX algorithm. *Journal of Applied Crystallography*, **41**, 1024–1037, doi: 10.1107/S0021889808030112.

HIELSCHER, R., SCHAEBEN, H. & SIEMES, H. 2010. Orientation distribution within a single hematite crystal. *Mathematical Geosciences*, **42**, 359–375.

HILL, R. 1952. The elastic behaviour of a crystalline aggregate. *Proceedings of the Physical Society A*, **65**, 349–354.

HOFER, M. & SCHILLING, F. R. 2002. Heat transfer in quartz, orthoclase, and sanidine. *Physics and Chemistry of Minerals*, **29**, 571–584.

HUMBERT, M. & DIZ, J. 1991. Some practical features for calculating the polycrystalline elastic properties from texture. *Journal of Applied Crystallography*, **24**, 978–981.

ISAAK, D. G. 2001. Elastic properties of minerals and planetary objects. *In*: LEVY, M., BASS, H. & STERN, R. (eds) *Handbook of Elastic Properties of Solids, Liquids, and Gases, Volume III: Elastic Properties of Solids: Biological and Organic Materials, Earth and Marine Sciences*. Academic Press, New York, 325–376.

JONES, M. N. 1985. *Spherical Harmonics and Tensors for Classical Field Theory*. Research Studies Press, Letchworth, England. 230.

KNEER, G. 1965. Über die berechnung der elastizitätsmoduln vielkristalliner aggregate mit texture. *Physica Status Solidi*, **9**, 825–838.

MAINPRICE, D. 1990. An efficient FORTRAN program to calculate seismic anisotropy from the lattice preferred orientation of minerals. *Computers & Geosciences*, **16**, 385–393.

MAINPRICE, D. 2007. Seismic anisotropy of the deep Earth from a mineral and rock physics perspective. *In*: SCHUBERT, G. (ed.) *Treatise in Geophysics*. Elsevier, Oxford, **2**, 437–492.

MAINPRICE, D. & HUMBERT, M. 1994. Methods of calculating petrophysical properties from lattice preferred orientation data. *Surveys in Geophysics*, **15**, 575–592.

MAINPRICE, D., LE PAGE, Y., RODGERS, J. & JOUANNA, P. 2008. *Ab initio* elastic properties of talc from 0 to 12 GPa: interpretation of seismic velocities at mantle pressures and prediction of auxetic behaviour at low pressure. *Earth and Planetary Science Letters*, **274**, 327–338, doi: 10.1016/j.epsl.2008.07.047.

MORRIS, P. R. 2006. Polycrystalline elastic constants for triclinic crystal and physical symmetry. *Journal of Applied Crystallography*, **39**, 502–508.

NYE, J. F. 1985. *Physical Properties of Crystals: Their Representation by Tensors and Matrices*. 2nd edn., Oxford University Press, England.

REUSS, A. 1929. Berechnung der Fließrenze von Mischkristallen auf Grund der Plastizitätsbedingung für Einkristalle. *Zeitschrift für angewandte Physik*, **9**, 49–58.

SANDER, B. 1911. Über Zusammenhänge zwischen Teilbewegung und Gefüge in Gesteinen. *Tschermaks Mineralogische und Petrographische Mitteilungen*, **30**, 381–384.

SIROTIN, Yu. I. & SHAKOLSKAYA, M. P. 1982. *Fundamentals of Crystal Physics*. Mir, Moscow, 654.

VAN DEN BOOGAART, K. G. 2001. *Statistics for individual crystallographic orientation measurements*. PhD Thesis, Shaker, Freiburg University of Mining & Technology.

VARSHALOVICH, D. A., MOSKALEV, A. N. & KHERSONSKII, V. K. 1988. *Quantum Theory of Angular Momentum*. World Scientific Publishing Co., Singapore.

VOIGT, W. 1887. Theoretische studien über die elastizitätsverhältnisse. *Abhandlungen der Akademie der Wissenschaften in Göttingen*, **34**, 48–55.

VOIGT, W. 1928. *Lehrbuch der Kristallphysik*. Teubner-Verlag, Leipzig.